CO-Free Hydrogen Production for Fuel Cell Applications over Au/CeO2 Catalysts: FTIR Insight into the Role of Dopant

ARTICLE *in* THE JOURNAL OF PHYSICAL CHEMISTRY A · SEPTEMBER 2009

Impact Factor: 2.69 · DOI: 10.1021/jp906892q · Source: PubMed

CO-Free Hydrogen Production for Fuel Cell Applications over Au/CeO_2 Catalysts: FTIR Insight into the Role of Dopant†

Tatyana Tabakova,*,‡ Maela Manzoli,§ Floriana Vindigni,§ Vasko Idakiev,‡ and Flora Boccuzzi§

Institute of Catalysis, Bulgarian Academy of Sciences, Acad. G. Bonchev Str., bl. 11, 1113 Sofia, Bulgaria, and Department of Inorganic, Physical and Materials Chemistry and NIS Centre of Excellence, University of Turin, via P. Giuria 7, 10125 Turin, Italy

Received: July 21, 2009; Revised Manuscript Received: September 8, 2009

The impact of ceria doping by Zn (atomic ratio $Zn/(Zn + Ce) = 0.05$) on the structural and catalytic properties of Au/CeO_2 catalyst was studied. The ceria modification influenced the catalytic activity toward purification of hydrogen via water−gas shift (WGS) and preferential CO oxidation (PROX) reactions in a different way: it diminished the WGS activity and improved the PROX performance. A characterization by FTIR spectroscopy was conducted to explain differences in the catalytic performance. The nature of gold active species after different pretreatments, under different atmospheres (H_2, D_2), and after admission of CO and its subsequent interaction with $^{18}O_2$ was investigated. Evidence has been found of the dissociation of hydrogen at room temperature on gold, producing on the oxidized sample a broad absorption assigned to Au−OH vibrations, whereas on the reduced one, bands at 3200 and 1800 cm^{-1} ascribed, respectively, to Au−OH and Au−H species have been detected. For the first time, the formation of Au−hydride on supported heterogeneous catalysts was proposed. These features were stronger on the Au/CeO_2 sample than on the $Au/Zn-CeO_2$ sample. The availability of highly dispersed gold clusters in contact with oxygen vacancies on the ceria surface could contribute to higher WGS activity, whereas the steps of small gold particles are the active sites for both CO and oxygen activation during the PROX reaction.

1. Introduction

Environmental protection and energy security are very important challenges that people face nowadays. Technological advances in the application of hydrogen fuel cells in both transport and energy sectors are possible solutions. In the past decade, research has demonstrated the very high potential of fuel cells to replace the internal combustion engine in vehicles and to provide power in stationary and portable power applications because they are energy-efficient, clean, and fuel-flexible.[1–3] Together, hydrogen and fuel cells represent a radically different approach to energy conversion. Hydrogen has great potential as an environmentally clean, renewable, and highly efficient energy carrier. Nowadays, hydrogen is mostly produced from fossil fuels by a multistep process that includes catalytic reforming or autothermal reforming of hydrocarbons, followed by water−gas shift (WGS) reaction ($CO + H_2O \leftrightarrow CO_2 + H_2$).[4,5] This reaction has a long historical application as an industrially important process for hydrogen production. In the past years, it has attracted renewed interest because of the increasing demands for high-purity hydrogen. The hydrogen-rich gas stream after the WGS reaction typically contains 0.5 to 1 vol % CO. Because of the high sensitivity of platinum anode electrode in polymer electrolyte membrane fuel cells (PEMFCs) toward even low level of CO, the concentration of CO should be reduced to <10 ppm. The catalytic selective oxidation of CO in hydrogen-rich gas stream known as the preferential oxidation (PROX) reaction appears to be the simplest and most cost-effective method for this purpose.[6–8] Both WGS and PROX reactions are important process steps in one very attractive approach to CO-free hydrogen production for fuel cell applications.

The development of fuel cell technology has focused considerable research interest on the design of active, stable, and poison-resistant catalysts for low-temperature WGS reaction as well as active and highly selective catalysts for PROX. Precious metal catalysts are often investigated because of their potential stability in oxidizing atmosphere. Supported gold catalysts have been extensively studied during the last two decades in view of their high WGS activity at low temperature.[9–16] Recent investigations have revealed the beneficial application of ceria as a support of active catalysts for the WGS reaction. The distinct defect chemistry of ceria and its ability to exchange lattice oxygen with the gas phase results in an oxide with unique catalytic properties, including the promotion of the precious metal dispersion and the enhancement of the catalytic activity at the interfacial metal−support sites.[17] Numerous studies of Au/CeO_2 catalysts have addressed how various factors, including method of preparation, gold loading and support surface area, gold particle size, structure and oxidation state, nature of the active gold species, and reactivity of surface species correlate with catalytic performance in the WGS reaction.[18–28] Gold/ceria catalysts have recently been proposed to be promising for the PROX reaction, too.[7,29–33] Comparative study of catalytic performance of gold and copper catalysts supported on ceria has revealed that Au/CeO_2 catalysts are significantly more active than CuO/ceria ones.[34] However, the presence of CO_2 and H_2O caused a decrease in the catalytic activity of the gold catalyst. The modification of ceria is an appropriate way to solve the problem of the stability under operating conditions. It is known that the incorporation of some additives in the ceria lattice could

† Part of the special issue "Green Chemistry in Energy Production Symposium".

* Corresponding author. Tel: (+359 2) 979 2528. Fax: (+359 2) 971 2967. E-mail: tabakova@ic.bas.bg.

‡ Bulgarian Academy of Sciences.

§ University of Turin.

10.1021/jp906892q
Published on Web 09/29/2009

enhance PROX activity because of the improved ceria oxygen mobility and thermal stability.[35–38] A very recent study of physicochemical properties and catalytic performance in the PROX reaction of nanosized gold supported on doped-ceria (dopant = Sm, La, Zn) has demonstrated that the Zn-doped Au/ceria catalyst was more active than the undoped one and showed improved resistance toward deactivation by CO_2.[39] Moreover, coaddition of CO_2 and H_2O counteracted the negative effect of CO_2.

The behavior of these Au/doped ceria catalysts was evaluated in the WGS reaction. In particular, Au/Zn−CeO_2 attracted our interest in view of its performance in the PROX reaction. The aim of this work was to gain further insight into the factors that influence the catalytic performance of Au/CeO_2 and Au/Zn−CeO_2 for PROX and WGS reactions. We tried to find experimental evidence to explain how a slight ceria modification is able to change the catalytic properties significantly. We focused on the characterization by FTIR spectroscopy as a very useful tool to get information on the nature of gold active species after different pretreatments, under different atmospheres (H_2, D_2), and after admission of CO and its subsequent interaction with $^{18}O_2$.

2. Experimental Section

2.1. Materials. Au/CeO_2 and Au/Zn-doped CeO_2 catalysts were prepared by deposition−precipitation, as described elsewhere.[39] In brief, Zn-doped ceria support was synthesized by a coprecipitation of mixed aqueous solutions of nitrate salts of cerium and zinc with K_2CO_3 (atomic ratio Zn/(Zn + Ce) = 0.05) at constant pH 9.0 and temperature = 333 K. The precipitate was aged for 1 h at 333 K, filtered, washed carefully until absence of NO_3^- ions, dried under vacuum at 353 K, and calcined in air at 673 K for 2 h. The same procedure was used for the preparation of pure ceria. Gold hydroxide was deposited onto the supports through a chemical interaction between $HAuCl_4 \cdot 3H_2O$ (Merck) and K_2CO_3 at constant pH 7.0 and temperature 333 K and further aging, washing, drying, and calcination, as in the case of supports' preparation. The actual gold loading for each catalyst was 3 (±0.05) wt %, as measured by AAS.

2.2. Techniques. Various characterization techniques were used for physicochemical characterization of the catalysts (BET, HRTEM, XRD, TPR), and they were already reported in detail.[39] In this investigation, we collected new supplementary FTIR spectra on a Perkin-Elmer 1760 spectrometer (equipped with a MCT detector) with the samples in self-supporting pellets introduced in a cell allowing thermal treatment under controlled atmospheres. The catalysts were submitted to an oxidative treatment and in some cases followed by a reductive treatment. The oxidative treatment included heating from room temperature (RT) to 473 K under outgassing; an inlet of 40 mbar of oxygen, and heating up to 673 K; at 673 K, the oxygen was changed three times (40 mbar for 10 min each one). After that, the sample was cooled to RT in oxygen and finally outgassed at the same temperature. The reductive treatment was carried out after the oxidation by heating from RT under 20 mbar of H_2; at the temperature selected for reduction, the hydrogen was changed two times (20 mbar for 10 min each one), and after that the sample was cooled to RT under outgassing. Band integration was carried out by "Curvefit" in Spectra Calc (Galactic Industries) by means of Lorentzian curves.

The WGS activity measurements were carried out in a flow reactor under atmospheric pressure. The reactant gas mixture fed into the reactor contained 4.42 vol % CO with the rest being argon. The following conditions were applied: catalyst bed volume = 0.5 cm^3 (0.63 to 0.80 mm pellets), space velocity = 4000 h^{-1}, partial pressure of water vapor = 31.1 kPa. The analysis of the mixture converted at the reactor outlet was carried out on an "URAS-3G" (Hartmann & Braun AG) gas analyzer with respect to the CO content. The catalytic activity was expressed by the degree of CO conversion.

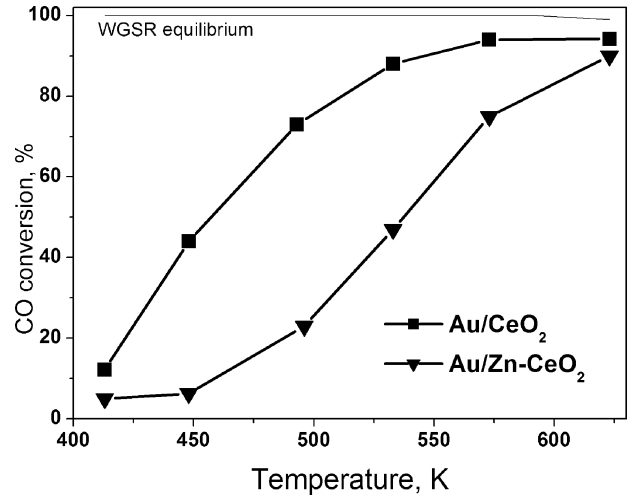

Figure 1. Temperature dependence of the CO conversion in the WGS reaction on different catalysts.

3. Results and Discussion

3.1. Catalytic Properties. Very recently, in a detailed study of gold supported on doped ceria catalysts, a positive effect of doping with Zn^{2+} on the catalytic performance in the PROX reaction has been demonstrated.[39] Under standard experimental conditions (W/F = 0.03 g s cm^{-3}, where W is the weight of catalyst and F is the total flow rate of the reactant gas), the maximum CO conversion achieved over the Zn-doped and the undoped Au/ceria catalysts was 96 (with 40% selectivity) and 88% (with 37% selectivity) at 363 K. In contrast with the PROX activity enhancement after ceria modification, a significant decrease in activity for the WGS reaction was observed over Au/Zn−CeO_2 over the whole temperature range. The temperature dependence of CO conversion in the course of the WGS reaction over Au/CeO_2 and Au/Zn−CeO_2 catalysts is illustrated in Figure 1. The comparison of the CO conversion curves revealed that the doping of ceria by Zn diminished the activity in the WGS reaction. The activity of Zn-doped gold catalyst was lower than that of undoped Au/CeO_2. This catalytic behavior was quite unexpected because the addition of divalent or trivalent ions to ceria usually causes increased oxygen mobility and vacancy formation that correlate with better catalytic activity. Because of the important role of gold particle size on catalytic activity, we will shortly recall that HRTEM images of Au/CeO_2 evidenced the presence of both big gold particles with size of at least 10 nm and very highly dispersed gold clusters with size of about 1 nm, whose presence on the surface was confirmed by EDS analysis. Gold particles were hardly detected on Au/Zn−CeO_2, indicating that the gold dispersion is high and more homogeneous. In the FTIR spectra (Figure S1 in the Supporting Information) collected after CO adsorption at 90 K on the catalysts previously subjected to oxidation at 673 K and subsequent evacuation, an absorption band centered at 2101 cm^{-1} in Au/Zn−CeO_2 was observed, whereas a weak band at 2104 cm^{-1} was detected in the case of Au/CeO_2. Both bands were assigned to CO adsorption on Au^0 step sites of gold

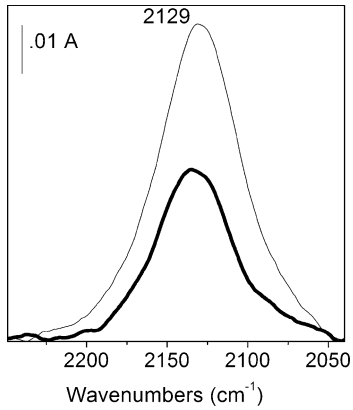

Figure 2. FTIR absorbance spectra of reduced Au/CeO_2 (fine curve) and $Au/Zn-CeO_2$ (bold curve). The spectra have been normalized to the weight of the pellets.

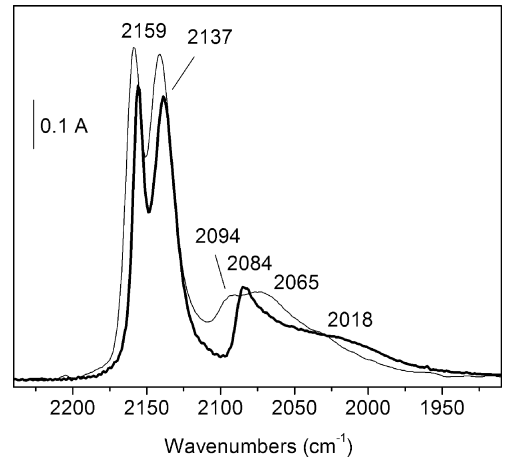

Figure 3. FTIR absorption spectra after admission of 3.5 mbar CO at 90 K on reduced at 423 K Au/CeO_2 (fine curve) and $Au/Zn-CeO_2$ (bold curve).

nanoparticles. However, their intensity order, $Au/Zn-CeO_2$ (2.08) > Au/CeO_2 (0.67), revealed a different abundance of small metallic gold particles on the surface. In particular, the relative intensities of these bands were in agreement with HRTEM analysis, which indicated Au particles with size ≥10 nm together with highly dispersed clusters of ∼1 nm on Au/CeO_2. The very weak absorption in the region corresponding to CO on gold sites for Au/CeO_2 was explained by considering that the big particles expose only a minimal amount of step sites (the only ones able to adsorb CO), whereas the small gold clusters ($d \leq$ 1 nm) are covered by adsorbed oxygen after the calcination pretreatment.[40] At the same time, the higher intensity of the band at 2101 cm^{-1} was an indication that small gold particles instead of clusters are predominantly available on the surface of $Au/Zn-CeO_2$. The already summarized HRTEM data and the FTIR results that will be discussed in a later section focus on the importance of gold clusters for the WGS activity of Au−ceria catalytic systems.

3.2. FTIR Measurements. ***3.2.1. Abundance of Defect Sites of the Reduced Gold Catalysts.*** The absorbance spectra of Au/CeO_2 (fine curve) and $Au/Zn-CeO_2$ (bold curve) after normalization to the weight of the pellets are shown in Figure 2. The band at 2129 cm^{-1} was related to the forbidden $^2F_{5/2} \rightarrow {}^2F_{7/2}$ electronic transition of Ce^{3+} and gives information for the presence of defects at the ceria surface. This comparison demonstrated that the concentration of Ce^{3+} defective sites, associated with oxygen vacancies, is higher on the surface of Au/CeO_2 than on Au/Zn-doped ceria. This trend correlates well with the experimental WGS activity data and additionally confirms the important role of O vacancies on ceria for high WGS activity.[41,42] At the same time, it is opposite from that concerning catalytic results for the PROX reaction, where an enhancement by Zn-doping was observed.

3.2.2. Nature and Abundance of Gold Sites on Reduced Samples by FTIR Absorption Spectra of CO. Several recent researches, both theoretical calculations and experimental results, have discussed the impact of gold particle size and oxidation state on the WGS activity of Au/CeO_2 catalysts. The suggestions for the active charge of gold vary between neutral[21,22,41,43] and positive.[42,44,45] The conclusions that the oxidation state of Au changes with the composition of the reaction mixture[43,46] as well as after pretreatment of the catalyst under different atmospheres are probably more relevant.[47] However, as concerns the gold particle size, there is consensus of opinion that small Au clusters are those that demonstrate high WGS activity over Au/CeO_2.[21,23,42−44] The spectra collected after adsorption of CO on the catalysts reduced at 423 K are compared in Figure 3. The reduction temperature was chosen considering that the WGS reaction started at temperature >400 K. The admission of CO at 90 K gives rise to two bands related to the formation of carbonyls with the support sites at 2159 and 2142 cm^{-1} in the spectrum of Au/CeO_2 and at 2155 and 2137 cm^{-1} in that of $Au/Zn-CeO_2$, respectively. The former two bands in each spectrum (at 2159 and 2155 cm^{-1}) are due to CO on Ce^{4+} sites, whereas the latter are ascribed to CO on Ce^{3+} sites, formed during the reduction. A broad and complex absorption at 2065 cm^{-1}, which was strongly red-shifted with respect to the usual position of CO adsorbed on Au^0 step sites at 2100 cm^{-1}, was observed in the spectrum of undoped Au/CeO_2 (fine curve). This band was assigned to CO on gold clusters, which was negatively charged because of an electronic transfer from the reduced support to gold, as previously reported by some of us.[21] In the case of $Au/Zn-CeO_2$ (bold curve), the band was narrower than that of Au/CeO_2, with a more asymmetric shape and a well-defined maximum at 2084 cm^{-1}. Additionally, the appearance of a new component at 2018 cm^{-1} in this band that is significantly red-shifted and that can be assigned to CO adsorbed on gold exposed at the surface of $Au-Ce_x$ particles should be pointed out. The different charge of the dopant (Zn^{2+}) could cause a higher reducibility of ceria, with possible formation of $Au-Ce_x$ alloy clusters. Zhao et al. have reported photoemission and STM studies for the adsorption and dissociation of water on Ce−Au(111) alloys and found that $CeAu_2$/Au(111) alloys exhibit a relatively low reactivity toward water.[48] The dissociation of H_2O is a crucial step in the WGS reaction. The formation of $Au-Ce_x$ alloy clusters could be the reason for the depletion of oxygen vacancies, for the diminished ability in water activation, and, consequently, for the decreased WGS activity over $Au/Zn-CeO_2$.

Spectroscopic evidence of the effect of the support composition on the catalytic activity in the PROX reaction is reported in Figure 4, where the evolution of the bands during CO and $^{18}O_2$ interaction on the $Au/Zn-CeO_2$ sample within 20 min is shown. (The temperature of reduction pretreatment, 373 K, was chosen considering the temperature region for the operation of the catalyst in the PROX reaction.[39]) The analysis of the spectra collected on $Au/Zn-CeO_2$ showed that a rapid exchange between the oxygen of ceria and the $^{18}O_2$ molecules coming from the gas phase occurs already at 90 K. The inlet of $^{18}O_2$ at increasing diffusion times over the sample previously saturated by CO at 90 K (green curve) caused strong erosion from the low-frequency side of the band at 2095 cm^{-1}. After the $^{18}O_2$

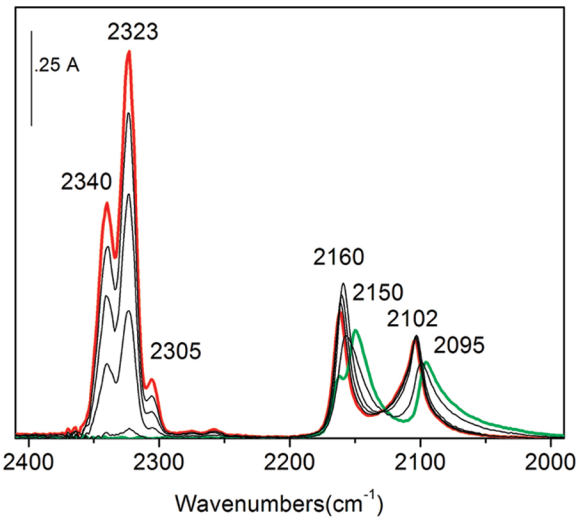

Figure 4. Evolution of FTIR absorbance spectra at 90 K after the inlet of $^{18}O_2$ on preadsorbed CO on Au/Zn−CeO_2 reduced at 373 K (green curve) and after 20 min (red curve).

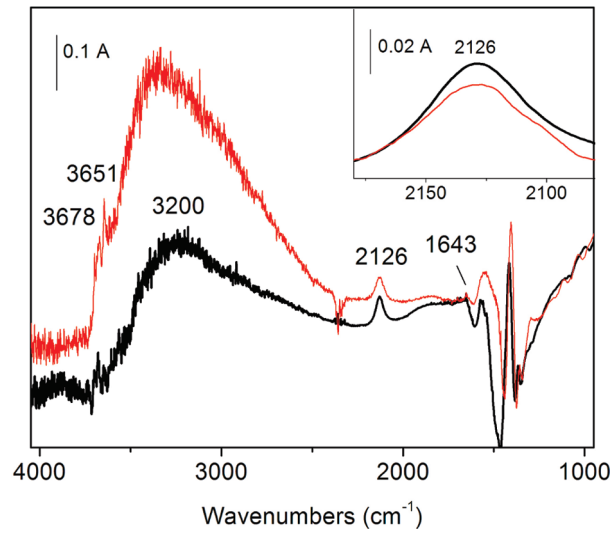

Figure 5. Comparison of the difference spectra collected 2.5 h after the inlet of 50 mbar H_2 on oxidized Au/CeO_2 (black curve) and Au/Zn−CeO_2 (red curve).

interaction at 90 K, the band shifted from 2095 to 2102 cm^{-1}, and it appeared to be narrow and with a maximum in the usual position of CO adsorbed on the Au^0 sites. The band at 2150 cm^{-1} disappeared, and a new band at 2160 cm^{-1} related to CO adsorbed on Ce^{4+} sites was produced. The main aim of this experiment was to compare the bands at higher frequencies, namely, those related to CO_2 formation, during the CO oxidation on Au/Zn−CeO_2 and Au/CeO_2. Three isotopomers of CO_2 were registered in the spectra of Au/Zn−CeO_2 (red curve): a growing band at 2323 cm^{-1}, assigned to the $C^{16}O^{18}O$ solid-like phase, accompanied by weaker bands at 2340 and at 2305 cm^{-1}, assigned to $C^{16}O_2$ and $C^{18}O_2$ solid-like phase, respectively.[49] The high intensity of the band ascribed to $C^{16}O^{18}O$ indicated that oxygen participating in the reaction at 90 K mainly comes from the gas phase. At the same time, the appearance of the band at 2340 cm^{-1} evidenced the fact that the modification with Zn led to increased oxygen mobility because of improved exchange properties of ceria support. This result demonstrated the enhanced ability of doped-ceria support to supply active lattice oxygen that is beneficial for the PROX reaction. Here we recall that these experiments were performed on catalysts reduced at 373 K, that is, the temperature of optimum performance for the PROX reaction. In the spectra of Au/CeO_2 (Figure S2 in the Supporting Information), only a band at 2323 cm^{-1} was observed, suggesting that oxygen atoms of undoped ceria do not participate in the reaction. The presence of a multiplet of bands in the CO_2 stretching region after CO interaction with $^{18}O_2$ over Au/Zn−CeO_2, unlike over Au/CeO_2, clearly reveals that the doping of ceria by Zn facilitates the exchange reaction with the oxygen atoms of the support.

3.2.3. FTIR Absorption Spectra of Hydrogen Interaction on Differently Pretreated Catalysts. To clarify different performances of the studied catalysts in the WGS and PROX reactions better, FTIR experiments at RT in the presence of hydrogen were carried out. In Figure 5, the difference spectra collected 2.5 h after inlet of 50 mbar H_2 (reference spectra being those immediately after admission of hydrogen) of both studied catalysts, preliminary submitted to oxidation pretreatment, were compared. The spectroscopic features of the spectra were very similar. We focused on the appearance of two bands, namely, those at 2126 and 3200 cm^{-1}. They originated from reactions at RT because of the hydrogen dissociation.[50] The dissociated hydrogen atoms interact with oxygen, and Au−OH groups are formed. Furthermore, the creation of Ce^{3+} occurs to compensate for the reduced negative charge. The higher intensity of the broad band in the OH stretching region in the spectrum of Au/Zn−CeO_2 agreed with microscopic peculiarities that revealed the distribution of gold mainly as small particles able to dissociate hydrogen. Gold is deposited on Au/CeO_2 mostly as clusters covered with oxygen after oxidative treatment, which hampered interaction with hydrogen. The bands at 2126 cm^{-1} are shown in the inset. (See Figure 5.) A higher intensity was observed in the spectrum of Au/CeO_2 in the same way as was already reported in Figure 2. This comparison evidenced again a higher concentration of defect sites created on the surface of Au/CeO_2, and their contribution to the better WGS activity could be suggested.

A band at 2126 cm^{-1}, which indicated the effectiveness of the reduction, was observed in the spectra of reduced Au/CeO_2 (Figure S3 in the Supporting Information). The reduction treatment was performed at 473 K, taking into account the temperature window for operation of LT-WGS catalysts. Additionally, the reduction led to the OH groups' formation on the support surface, as evidenced by the broad band in the 4000−3000 cm^{-1} range with a maximum at ∼3200 cm^{-1}. The presence of free OH groups was confirmed by the weak band at 3651 cm^{-1}. The admission of 50 mbar hydrogen on Au/CeO_2 at increasing contact times produced the features illustrated in Figure 6. A gradual increase in the intensity of the absorption in the OH stretching range with a well-defined maximum at 3200 cm^{-1} depending on the contact time (up to 3 h) was produced. The intensity of the band at 2126 cm^{-1} was also increased. Moreover, a band at 1800 cm^{-1} grew up, and a monotonous absorption in the low-frequency range was observed. All of these features were related to the occurrence of hydrogen dissociation on gold at RT. Hydrogen atoms interact with Au−O and Au^0 sites, producing Au−OH (bands at 3660 and 3200 cm^{-1}, free and H-bonded, respectively) and Au−H species (band at 1800 cm^{-1}). By using DFT calculations Hernandez et al. have shown that gold atoms at a ceria (111) surface can adopt several oxidation states, depending on the site of adsorption.[51] A charge transfer from the gold atom to one of the Ce cations at the surface could occur if gold is located on top of the surface oxygen or bridged between two surface oxygen atoms, resulting in the electronic configurations Au^+

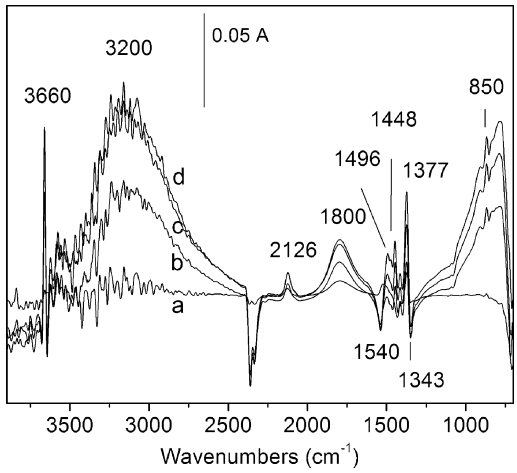

Figure 6. Evolution of the spectra after admission of H_2 (50 mbar) on reduced Au/CeO_2 (curve a) and after 3 h (curve d).

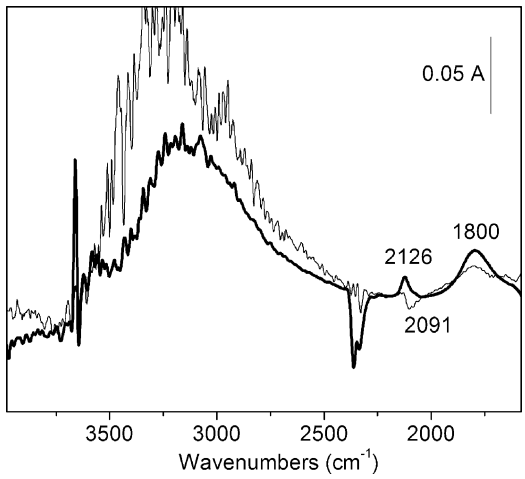

Figure 7. Comparison of spectra collected 3 h after admission of H_2 (50 mbar) on reduced catalysts: Au/CeO_2 (bold curve) and $Au/Zn-CeO_2$ (fine curve).

and Ce^{3+}, whereas the location near an oxygen vacancy leads to electronic configuration of an Au^-. Additionally, an Au−OH absorption band at a similar frequency has already been observed by Quinet et al. in a study of H_2-induced promotion of CO oxidation over unsupported gold.[52] The formation of Au−OH was also suggested by some of us in a previous paper concerning gold on titania and iron oxide.[50] As for the Au−hydride, there are up to now no reports, as for the supported heterogeneous catalysts. However, this species has been extensively studied by theoretical calculations,[53,54] and recently, the structure of a stable gold(I)−hydride homogeneous complex was reported.[55] To verify the assignment of band at ∼1800 cm^{-1} to Au−hydride, we collected spectra after admission of D_2 on a sample preliminarily reduced in hydrogen or in deuterium. Unfortunately, the expected position of the Au−D band at ∼1300 cm^{-1} (frequency ratio for isotopic counterparts 1.384) falls in the region of carbonates absorption, and an increment due to Au−deuteride formation could not be discerned.

The comparison of the difference spectra collected 3 h after inlet of H_2 on reduced catalysts showed that the modification of Au/CeO_2 by Zn caused some differences (Figure 7). The most visible one is the complete lack of the band at 2126 cm^{-1} and the appearance of a negative band at 2091 cm^{-1}. Usually, the depletion of the band at 2126 cm^{-1} is observed in an oxidative atmosphere and resulted from the disappearance of defects.

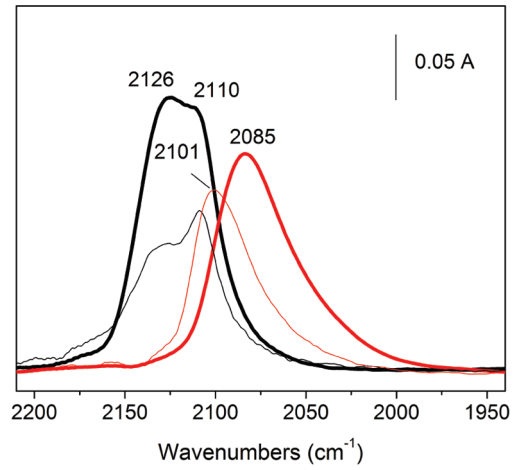

Figure 8. FTIR absorption spectra after the admission of 17 mbar CO at RT on the preliminary oxidized catalysts subjected to evacuation after inlet of 50 mbar H_2 (2.5 h) and CO_2 (1 h), Au/CeO_2 (black bold curve) and $Au/Zn-CeO_2$ (black fine curve), and on the preliminary reduced catalysts subjected to the same treatments as the oxidized ones, Au/CeO_2 (red bold curve) and $Au/Zn-CeO_2$ (red fine curve).

However, considering the reductive conditions in the IR cell, an assignment to healing of oxygen vacancies should be discarded. Moreover, a band with even slightly higher intensity than that in the spectrum of Au/CeO_2 in the OH stretching region indicated the interaction of dissociated hydrogen. We have already discussed the probable formation of Au−Ce alloy after the reduction of $Au/Zn-CeO_2$ at 423 K. This phenomenon could contribute to the observed decrease in the Ce^{3+} and, respectively, to the reduced number of oxygen vacancies, which is believed to be one of the reasons for the WGS activity. Additionally, a lower intensity of the band at 1800 cm^{-1} already ascribed to Au−hydride should be noted. The inclusion of a part of gold in alloy clusters could explain the diminished amount of Au−hydride species.

3.2.4. Nature and Abundance of Gold Sites on Preliminary Oxidized or Reduced Catalysts by FTIR Absorption Spectra of CO after Different Interactions. The FTIR spectra were collected after the admission of CO at RT on the catalysts subjected to treatments and different interactions, as described above. First, we will comment on the spectra produced by the admission of CO on the oxidized catalysts that were evacuated at RT after inlet of hydrogen (2.5 h) and subsequent interaction with CO_2 for 1 h. (The interaction of H_2 and CO_2 to simulate the reverse WGS reaction is not discussed in the present article.) Full-range spectra (4000−800 cm^{-1}, not shown) of both catalysts showed an increased adsorption in the carbonate region immediately after inlet of 17 mbar CO. At the same time, a well-defined band at ∼2127 cm^{-1} was registered in the carbonylic region of the spectrum of Au/CeO_2 (Figure 8, black bold curve). In fact, the inspection of the bands in the 2200−2000 cm^{-1} range revealed that the appearance of this band resulted from overlapping of two different components, centered at 2110 and 2126 cm^{-1}, related to two different gold species. The band at 2110 cm^{-1} was easily assigned, on the basis of previous works,[21,29,47,49] to CO adsorption on metallic gold nanoparticles. The band at 2126 cm^{-1} could be ascribed to CO adsorbed on cationic gold clusters $(Au_n)^{\delta+}$ that are formed after oxidation treatment.[21,56] The usual frequency range for the appearance of positively charged Au clusters is 2130−2180 cm^{-1}. The reason for the red shift observed in this study could be the treatment before the inlet of CO, that is, the interaction with hydrogen and CO_2 at RT. The red shift may be related to

the presence of the hydridic species on the small clusters that are able to reduce the positive charge of the clusters, and, consequently, the red shift of the coadsorbed CO occurs.

The band of CO in the spectrum of oxidized Au/Zn−CeO_2 (Figure 8, black fine curve) was more asymmetric, with a well-defined maximum at 2110 cm^{-1} and a broad and weaker shoulder at 2126 cm^{-1}. The assignment of the gold sites was the same as above, but the different shape of the complex band evidenced a different abundance of small gold particles and clusters located at the surface of both catalysts. The main fraction of gold able to interact with CO in Au/CeO_2 is deposited as clusters, whereas in Au/Zn−CeO_2, a larger amount of small gold particles is present. Additional information for the nature of gold sites was received after the evacuation of CO (Figure S4 in the Supporting Information). The band at 2126 cm^{-1} showed irreversibility due to the stronger bond OC−$Au^{\delta+}$ in comparison to OC−Au^0 at 2110 cm^{-1} that is gradually depleted under outgassing at RT.

Similarly, the reduced catalysts were subjected to evacuation after admission of 50 mbar H_2 for 3 h (experiments commented in Figures 6 and 7) and then to interaction with CO_2 for 1 h. The inlet of 17 mbar CO was carried out at RT, and the spectra were compared in Figure 8 (red curves). A band with a maximum at 2085 cm^{-1} was observed in the spectrum of Au/CeO_2 (bold red curve). The band was already assigned to CO adsorbed on very small gold clusters, negatively charged as a consequence of an electron transfer from the reduced supports to the small clusters. The position and the intensity of the band indicated the stability of the dispersion of gold; no sintering of gold occurred. Small gold clusters preserved their size after thermal treatments and the following reverse WGS reaction. Looking at the position of the band centered at 2101 cm^{-1}, originated from the admission of CO on Au/Zn−CeO_2 (fine red curve), we could infer that the main part of gold is deposited as very small metallic particles. The data, reported in Figure 8, are an additional indication for the known property of ceria to keep a high and stable dispersion of noble metals. They also agreed with HRTEM observation and contributed to the elucidation of catalytic performance of Au/CeO_2 catalysts for WGS and PROX reactions.

4. Conclusions

The catalytic behavior of Au/CeO_2 and Au/Zn−CeO_2 in the WGS reaction was evaluated and compared with the performance of these catalysts for the PROX reaction. Au/CeO_2 demonstrated superior WGS activity, whereas Au/Zn−CeO_2 was more active for the PROX. The FTIR study combined with recent HRTEM measurements allowed us to clarify the reasons for the different behavior of both catalysts. Spectroscopic data collected after carrying out the experiments on catalysts and reduced at temperatures relevant for WGS and PROX reactions evidenced that (i) gold able to interact with CO is deposited as highly dispersed clusters of about 1 nm on the surface of Au/CeO_2, whereas small gold particles are predominantly available on the surface of Au/Zn−CeO_2 and (ii) the concentration of Ce^{3+} defective sites, associated with oxygen vacancies, is higher on the surface of Au/CeO_2 than on Au/Zn−CeO_2. Modification of ceria by Zn probably causes the formation of Au−Ce_x alloy clusters over a reasonable WGS reaction temperature region. These alloy clusters could be responsible for the depletion of oxygen vacancies and diminished ability in the water activation. By FTIR experiments with $^{18}O_2$, an enhanced supply of active lattice oxygen during the CO + O_2 interaction was observed on Zn-doped ceria reduced at 373 K. The findings of this study provide additional evidence of the previous proposition that gold clusters and Ce^{3+} defects are the active sites in the WGS reaction, whereas the step sites of gold particles are the active sites for both CO and oxygen activation and play a decisive role in the PROX reaction.

Acknowledgment. T.T. gratefully acknowledges financial support "Progetto Lagrange-Fondazione CRT" provided by the ISI Foundation, Turin, Italy.

Supporting Information Available: Comparison of FTIR spectra and evolution of FTIR absorbance spectra. This information is available free of charge via the Internet at http://pubs.acs.org.

References and Notes

(1) Choudhary, T. V.; Goodman, D. W. *Catal. Today* **2002**, *77*, 65.
(2) Ghenciu, A. F. *Curr. Opin. Solid State Mater. Sci.* **2002**, *6*, 389.
(3) Cheekatamarla, P. K.; Finnerty, C. M. *J. Power Sources* **2006**, *160*, 490.
(4) Trimm, D. L. *Appl. Catal., A* **2005**, *296*, 1.
(5) Ruettinger, W.; Liu, X.; Farrauto, R. J. *Appl. Catal., B* **2006**, *65*, 135.
(6) Avgouropoulos, G.; Ioannides, T.; Papadopoulou, Ch.; Batista, J.; Hocevar, S.; Matralis, H. *Catal. Today* **2002**, *75*, 157.
(7) Ko, E. Y.; Park, E. D.; Seo, K. W.; Lee, H. C.; Lee, D.; Kim, S. *Catal. Today* **2006**, *116*, 377.
(8) Jung, C. R.; Kundu, A.; Nam, S. W.; Lee, N. I. *Appl. Catal., B* **2008**, *84*, 426.
(9) Andreeva, D.; Idakiev, V.; Tabakova, T.; Andreev, A. *J. Catal.* **1996**, *158*, 354.
(10) Sakurai, H.; Ueda, A.; Kobayashi, T.; Haruta, M. *Chem. Commun.* **1997**, 271.
(11) Andreeva, D. *Gold Bull.* **2002**, *35*, 82.
(12) Luengaruemitchai, A.; Osuwan, S.; Gulabi, E. *Catal. Commun.* **2003**, *4*, 215.
(13) Hua, J.; Zheng, Q.; Zheng, Y.; Wei, K.; Lin, X. *Catal. Lett.* **2005**, *102*, 99.
(14) Bond, G. C.; Louis, C.; Thompson, D. T. *Catalysis by Gold*; Imperial College Press: London, 2006.
(15) Sandoval, A.; Gomez-Cortes, A.; Zanella, R.; Dıaz, G.; Saniger, J. M. *J. Mol. Catal. A: Chem.* **2007**, *278*, 200.
(16) Boaro, M.; Vicario, M.; Llorca, J.; de Leitenburg, C.; Dolcetti, G.; Trovarelli, A. *Appl. Catal., B* **2009**, *88*, 272.
(17) Trovarelli, A. *Catal. Rev.−Sci. Eng.* **1996**, *38*, 439.
(18) Fu, Q.; Weber, A.; Flytzani-Stephanopoulos, M. *Catal. Lett.* **2001**, *77*, 87.
(19) Andreeva, D.; Idakiev, V.; Tabakova, T.; Ilieva, L.; Falaras, P.; Bourlinos, A.; Travlos, A. *Catal. Today* **2002**, *72*, 51.
(20) Tabakova, T.; Boccuzzi, F.; Manzoli, M.; Andreeva, D. *Appl. Catal., A* **2003**, *252*, 385.
(21) Kim, C. H.; Thompson, L. T. *J. Catal.* **2005**, *230*, 66.
(22) Fu, Q.; Deng, W.; Saltsburg, H.; Flytzani-Stephanopoulos, M. *Appl. Catal., B* **2005**, *56*, 57.
(23) Jacobs, G.; Ricote, S.; Patterson, P. M.; Graham, U. M.; Dozier, A.; Khalid, S.; Rhodus, E.; Davis, B. H. *Appl. Catal., A* **2005**, *292*, 229.
(24) Leppelt, R.; Schumacher, B.; Plzak, V.; Kinne, M.; Behm, R. J. *J. Catal.* **2006**, *244*, 137.
(25) Denkwitz, Y.; Karpenko, A.; Plzak, V.; Leppelt, R.; Schumacher, B.; Behm, R. J. *J. Catal.* **2007**, *246*, 74.
(26) Burch, R. *Phys. Chem. Chem. Phys.* **2006**, *8*, 5483.
(27) Karpenko, A.; Leppelt, R.; Plzak, V.; Cai, J.; Chuvilin, A.; Schumacher, B.; Kaiser, U.; Behm, R. J. *Top. Catal.* **2007**, *44*, 183.
(28) Daly, H.; Ni, J.; Thompsett, D.; Meunier, F. C. *J. Catal.* **2008**, *254*, 238.
(29) Schubert, M. M.; Plzak, V.; Garche, J.; Behm, R. J. *Catal. Lett.* **2001**, *76*, 143.
(30) Goerke, O.; Pfeifer, P.; Schubert, K. *Appl. Catal., A* **2004**, *263*, 11.
(31) Deng, W.; De Jesus, J.; Saltsburg, H.; Flytzani-Stephanopoulos, M. *Appl. Catal., A* **2005**, *291*, 126.
(32) Luengnaruemitchai, A.; Osuwan, S.; Gulari, E. *Int. J. Hydrogen Energy* **2004**, *29*, 429.
(33) Arena, F.; Famulari, P.; Trunfio, G.; Bonura, G. *Appl. Catal., B* **2006**, *66*, 81.
(34) Avgouropoulos, G.; Papavasiliou, J.; Tabakova, T.; Idakiev, V.; Ioannides, T. *Chem. Eng. J.* **2006**, *124*, 41.

(35) Chang, L.; Sasirekha, N.; Chen, Y.; Wang, W. *Ind. Eng. Chem. Res.* **2006**, *45*, 4927.
(36) Tu, Y.-B.; Luo, J.-Y.; Meng, M.; Wang, G.; He, J.-J. *Int. J. Hydrogen Energy* **2009**, *343*, 3743.
(37) Wang, H.; Zhu, H.; Qin, Z.; Liang, F.; Wang, G.; Wang, J. *J. Catal.* **2009**, *264*, 154.
(38) Ilieva, L.; Pantaleo, G.; Ivanov, I.; Zanella, R.; Venezia, A. M.; Andreeva, D. *Int. J. Hydrogen Energy* **2009**, *34*, 6505.
(39) Avgouropoulos, G.; Manzoli, M.; Boccuzzi, F.; Tabakova, T.; Papavasiliou, J.; Ioannides, T.; Idakiev, V. *J. Catal.* **2008**, *256*, 237.
(40) Bondzie, V. A.; Parker, S. C.; Campbell, C. T. *Catal. Lett.* **1999**, *63*, 143.
(41) Wang, X.; Rodriguez, J. A.; Hanson, J. C.; Perez, M.; Evans, J. *J. Chem. Phys.* **2005**, *123*, 221101.
(42) Liu, Z.-P.; Jenkins, S. J.; King, D. A. *Phys. Rev. Lett.* **2005**, *94*, 196102.
(43) Tibiletti, D.; Amieiro-Fonseca, A.; Burch, R.; Chen, Y.; Fisher, J. M.; Goguet, A.; Hardacre, C.; Hu, P.; Thompsett, D. *J. Phys. Chem. B* **2005**, *109*, 22553.
(44) Fu, Q.; Saltsburg, H.; Flytzani-Stephanopoulos, M. *Science* **2003**, *301*, 935.
(45) Castellani, N. J.; Branda, M. M.; Neyman, K. M.; Illas, F. *J. Phys. Chem. C* **2009**, *113*, 4948.
(46) Deng, W.; Frenkel, A. I.; Si, R.; Flytzani-Stephanopoulos, M. *J. Phys. Chem. C* **2008**, *112*, 12834.
(47) Romero-Sarria, F.; Penkova, A.; Martinez, L. M.; Centeno, M. A.; Hadjiivanov, K.; Odriozola, J. A. *Appl. Catal., B* **2008**, *84*, 119.
(48) Zhao, X.; Ma, S.; Hrbek, J.; Rodriguez, J. A. J. *Surf. Sci.* **2007**, *601*, 2445.
(49) Boccuzzi, F.; Chiorino, A.; Manzoli, M.; Andreeva, D.; Tabakova, T. *J. Catal.* **1999**, *188*, 176.
(50) Boccuzzi, F.; Chiorino, A.; Manzoli, M.; Lu, P.; Akita, T.; Ichikawa, S.; Haruta, M. *J. Catal.* **2001**, *202*, 256.
(51) Hernandez, N. C.; Grau-Crespo, R.; de Leeuw, N. H.; Sanz, J. F. *Phys. Chem. Chem. Phys.* **2009**, *11*, 5246.
(52) Quinet, E.; Piccolo, L.; Daly, H.; Meunier, F. C.; Morfin, F.; Valcarcel, A.; Diehl, F.; Avenier, P.; Caps, V.; Rousset, J. L. *Catal. Today* **2008**, *138*, 43.
(53) Hashmi, A. S. K.; Hutchings, G. J. *Angew. Chem., Int. Ed.* **2006**, *45*, 7896.
(54) Pyycco, P. *Angew. Chem., Int. Ed.* **2004**, *43*, 4412.
(55) Tsui, E. Y.; Muller, P.; Sadighi, J. *Angew. Chem., Int. Ed.* **2008**, *47*, 8937.
(56) Mihaylov, M.; Gates, B. C.; Fierro-Gonzalez, J. C.; Hadjiivanov, K.; Knozinger, H. *J. Phys. Chem. C* **2007**, *111*, 2548.

JP906892Q